Morphological, Physiological, Biochemical, and Transcriptome Studies Reveal The Importance of Different Component Traits During Salinity Stress in *Prunus*

Biswa R. Acharya
University of California, Riverside
Devinder Sandhu (devinder.sandhu@usda.gov)
USDA-ARS US Salinity Laboratory
Christian Dueñas
University of California, Riverside
Marco Dueñas
University of California, Riverside
Manju Pudussery
USDA-ARS US Salinity Laboratory
Amita Kaundal
Utah State University
Jorge F.S. Ferreira
USDA-ARS US Salinity Laboratory
Donald L. Suarez
USDA-ARS US Salinity Laboratory
Todd H. Skaggs
USDA-ARS US Salinity Laboratory

Research Article

Keywords: Almond, Rootstock, Prunus, Peach, ‘Rootpac 40’, ‘Nemaguard’, RNA-Seq, Transcriptome, Gene expression, Salt stress, Salinity, Calcium, CBL10, Proline, Na, Cl, K, AKT1, and KUP8

Posted Date: July 7th, 2021

DOI: https://doi.org/10.21203/rs.3.rs-659140/v1

Abstract

The almond crop has high economic importance on a global scale but its sensitivity to salinity stress can cause severe yield losses. Salt-tolerant rootstocks are vital for crop economic feasibility under saline conditions. Two commercial rootstocks submitted to salinity, and evaluated through different parameters, had contrasting results with the survival rates of 90.6% for 'Rootpac 40' (tolerant) and 38.9% for 'Nemaguard' (sensitive) under salinity (Electrical conductivity of water = 3 dS m^{-1}). Under salinity, 'Rootpac 40' accumulated less Na and Cl and more K in leaves than 'Nemaguard'. Increased proline accumulation in 'Nemaguard' under salinity was an indicator of the high-stress levels compared to 'Rootpac 40'. RNA-Seq analysis revealed a higher degree of differential gene expression was controlled by genotype rather than by treatment. Differentially expressed genes (DEGs) provided insight into the regulation of salinity tolerance in *Prunus*. DEGs associated with stress signaling pathways and transporters may play essential roles for salinity tolerance in *Prunus*. Some additional vital players involved in salinity stress in *Prunus* include CBL10, AKT1, KUP8, *Prupe.3G053200* (chloride channel), and *Prupe.7G202700* (mechanosensitive ion channel). Genetic components involved in salinity stress identified in this study may be explored to develop new rootstocks suitable for salinity-affected regions.

Introduction

After drought, the most serious challenge facing agriculture and crop production is the looming issue of salinization of soil and water resources. Global climate change has led to more prolonged and severe droughts in many parts of the world[1], forcing growers to rely on low-quality water sources and utilize unsustainable irrigation and fertilization practices that increase soil salinization[2]. Saline soil disrupts plant homeostasis in many ways. For example, increases in soil salinity can cause changes in water potential that result in osmotic stress in plants[2]. Another consequence of excess soil salinity in the long run is ionic stress, resulting in an imbalance of necessary macro and micronutrients and disruption of metabolic processes, and triggers the production of toxic reactive oxidative species (ROS) in salt-stressed plants[3]. These and other salinity effects contribute to decreased productivity[4]. It has been estimated that salinization may impact as much as 50% of arable land by the year 2050, and worldwide economic losses from salinity stress are estimated to be over tens of billions U.S. dollars per year[5]. Thus, thorough knowledge of plant salinity tolerance is warranted to maintain crop production for both economic benefit and food supply.

Numerous studies utilizing model plants have been carried out to uncover molecular mechanisms of the plant response to salinity stress. In general, plants activate a signaling cascade in response to salt stress that leads to changes in gene expressions involved in various biochemical and physiological processes[3,6]. Some specific genes involved in salinity stress have been discovered. For instance, the salt overly sensitive (SOS) gene family members prevent Na^+ accumulation in plants, leading to increased salt tolerance[7,8]. Other genes of interest include the high-affinity potassium transporter (HKT) family members that aids in preventing root-to-shoot Na^+ movement, and sodium hydrogen exchanger (NHX)

transporters, found in the vacuoles of the plant cells that aid in maintaining ion homeostasis[9]. Though these findings provide a general foundation for studying plant salinity tolerance, it should be noted that plant response to salinity stress, including gene expression, varies considerably among species[10] and within species[11,12]. Information on these specific cases remains limited for non-model organisms, which is problematic as the effects of salinity on model plants may not entirely reflect the response of other plants[10].

Almond (*Prunus dulcis*) is an economically important crop in the United States, with over 80% of the world's almond production coming from California and contributing over 21.5 billion dollars to California's economy in 2014[13]. Many economic values and nutritional benefits stem from the consumption of almonds[14,15]. However, almond has the highest water footprint among major California crops on a per-unit and aggregate basis[16]. Considering that during the past drought in southern California, almond trees had to be eliminated because of insufficient irrigation water, the use of alternative waters, such as treated municipal wastewater, provides cheaper and tempting alternatives for irrigation. These waters have a slightly higher salt concentration than freshwater, representing a challenge for their use in a glycophytic C3 species that is sensitive to salinity stress, as almonds[17]. Root anatomical, cellular, and molecular traits have been investigated in three different almond rootstocks to study mechanisms of salinity tolerance at an early growth stage[18]. It has been shown that increasing electrical conductivity (EC) of watering solutions led to detrimental effects on the productivity of almonds, including a decrease in chlorophyll fluorescence, root and shoot growth[19]. Irrigation water with an electrical conductivity (EC_w) above 1.5 dS m^{-1} resulted in a halt in almond development and growth, with EC_w above 4 dS m^{-1} reducing growth by half[20]. The effect of excess salts also depends on the ionic composition of waters, not just the total salinity. When compared to 5 different saline water treatments, almond rootstocks grown under sodium/chloride-dominant waters had the highest reduction in survival rate and trunk diameter[21].

Rootstocks are critical for the success of an almond variety. Rootstocks provide a way to grow different almond cultivars in various soil conditions and mitigate specific stresses[21]. For example, the most widely used rootstock 'Nemaguard', a peach-based rootstock, is known for its high yields and resistance to root nematodes[22]. Previously, it was shown that the 'Nemaguard' *HKT1* ortholog was able to restore salinity tolerance in transgenic Arabidopsis *hkt1* mutants[23]. Varying levels of expression of more than 20 salt-stress responsive genes associated with Na^+ homeostasis (e.g. *SOS1*), K^+ homeostasis (e.g. *AKT1*), and Cl^- homeostasis (e.g. *SLAH1*) have been reported from a large-scale study involving over 14 different rootstocks and their response to salinity stress[21]. Although some individual genes are shown to be critical to salinity stress, the transcriptomic and metabolic effects of salinity stress are poorly understood in *Prunus*. Bioinformatic tools and techniques such as whole-genome sequencing and reference genomes have recently become readily available for the genus *Prunus*[24–26]. However, transcriptomic studies looking at genome-wide effects of salinity on *Prunus* rootstocks remain limited.

Previously, we conducted a preliminary screen of several almond rootstocks to evaluate their salinity tolerance and identified ‘Rootpac 40’ as the most salt-tolerant rootstock and ‘Nemaguard’ as the most salt-sensitive (data not shown). In this investigation, we performed phenotypic, physiological, and biochemical analyses to compare the salinity tolerance between two rootstocks; and conducted a 3-factor RNA sequencing (RNA-Seq) experiment using 2 levels per factor to test differential gene expression between the variables: rootstocks (‘Nemaguard’ and ‘Rootpac 40’), tissue type (leaf and root), and salinity treatment (control and salt treatment).

Results

Salinity Tolerance of ‘Rootpac 40’ and ‘Nemaguard’. To evaluate the salinity tolerance of ‘Rootpac 40’ and ‘Nemaguard’, rootstocks were irrigated with control irrigation water (1.36 dS m^{-1}) (C) and treatment irrigation water (3.0 dS m^{-1}) (T) for ten months (Table 1). The survival rate analysis revealed a higher survival rate for ‘Rootpac 40’ (90.6%) compared to ‘Nemaguard’ (38.9%) (Fig. 1a). The relative percent change of ‘Rootpac 40’ trunk diameter (58%) was slightly greater (*p*-value = 0.06) than that of ‘Nemaguard’ (45.5%) (Fig. 1b).

Table 1
Control and treatment irrigation water composition

Treatment	Salt composition
Control (C)	Non-saline control [Na^+ 1.65 $mmol_c\ L^{-1}$, K^+ 6.5 $mmol_c\ L^{-1}$, $PO4^{3-}$ 1.5 $mmol_c\ L^{-1}$, Mg^{2+} 1.3 $mmol_c\ L^{-1}$, SO_4^{2-}1.5 $mmol_c\ L^{-1}$, Cl^- 1.5 $mmol_c\ L^{-1}$, NO_3^- 5 $mmol_c\ L^{-1}$ and micronutrients]
Salinity Treatment (T)	Mixed cations (Ca^{2+} = 1.25 Mg^{2+} = 0.25 Na^+) with predominantly chloride (SO_4^{2-} = 0.2 Cl^-) [Na^+ 15.5 $mmol_c\ L^{-1}$, Ca^{2+}3.8 $mmol_c\ L^{-1}$, K^+ 6.5 $mmol_c L^{-1}$, PO_4^{3-}1.5 $mmol_c\ L^{-1}$, Mg^{2+}3.1 $mmol_c\ L^{-1}$, SO_4^{2-} 3.8 $mmol_c\ L^{-1}$, Cl^- 19 $mmol_c\ L^{-1}$, NO^{3-}5 $mmol_c\ L^{-1}$ and micronutrients]

Effect of salinity on biochemical responses. Proline content, antioxidant capacity (oxygen radical absorbance capacity, ORAC), and total phenolics in leaves of ‘Rootpac 40’ and ‘Nemaguard’ were evaluated under control and saline treatments (Fig. 1c and Supplemental Fig. S1). Our data indicated a comparable proline accumulation in the control and salinity treatments for ‘Rootpac 40’, but ‘Nemaguard’ showed a significant increase in proline concentration in response to salinity (Fig. 1c). There were no significant changes in antioxidant capacity in either ‘Nemaguard’ or ‘Rootpac 40’ in response to salinity treatment (Supplementary Fig. S1a). Similarly, neither ‘Nemaguard’ nor ‘Rootpac 40’, showed significant differences for total phenolics in response to salinity treatment (Supplementary Fig. 1b).

Effect of salinity on gas exchange parameters. To study how salt stress affects gas exchange parameters in 'Rootpac 40' and Nemaguad rootstocks, we evaluated chlorophyll content by Soil–Plant Analysis Development (*SPAD*) analysis, net photosynthetic rate (*Pn*), and leaf stomatal conductance (*gs*). Although *SPAD* analysis resulted in no significant effect of salinity on chlorophyll content on either rootstock, the average SPAD value was slightly smaller in 'Nemaguard' than in 'Rootpac 40' in both control and salt-treated rootstocks (Supplementary Fig. S2a). The photosynthetic efficiency (*Pn*) value analysis of 'Nemaguard' and 'Rootpac 40' indicated that salinity significantly inhibited photosynthesis in leaves of both rootstocks (Supplementary Fig. S2b). The stomatal conductance (*gs*) data revealed that salinity significantly affected stomatal conductance in 'Rootpac 40', but no significant effect was observed in 'Nemaguard', which had a high variation in *gs* values compared to 'Rootpac 40' (Supplementary Fig. S2c). However, it should be noted that, under salinity, 'Rootpac 40' and 'Nemaguard' had similar stomatal conductance values (Supplementary Fig. S2c).

Leaf ion accumulation in Rootstock 40 and 'Nemaguard' in response to salinity. To study ion accumulation characteristics of 'Rootpac 40' and 'Nemaguard' in response to salinity stress, ion analysis was performed on leaf samples for Na, Cl, K, Ca, Mg, P, S, B, Cu, Fe, Mn, Mo, and Zn (Fig. 1d,e,f, and Supplementary Fig. S3). In response to salinity stress, both rootstocks showed a higher accumulation of Na compared to their corresponding control. However, in response to salinity, 'Nemaguard' leaves accumulated over eight times the concentration of Na than that found in 'Rootpac 40' leaves (Fig. 1d). Both 'Rootpac 40' and 'Nemaguard' showed a significantly higher accumulation of leaf Cl in response to salinity but, similarly to what was observed for Na, the average accumulation of Cl in 'Nemaguard' leaves was 1.75-fold higher than that of 'Rootpac 40' (Fig. 1e). It is worth noting that under the control condition, 'Rootpac 40' showed 12-fold less Na accumulation and three-fold less Cl accumulation than 'Nemaguard'. Additionally, a significant increase in K accumulation was observed in 'Rootpac 40' in response to salinity, which also showed a treatment/control (T/C) K accumulation ratio of 1.14. However, a significant decrease in K accumulation in response to salt treatment was observed in leaves of 'Nemaguard' with a T/C ratio of 0.75 (Fig. 1f). There was no significant accumulation of Ca, Mg, S, B, Cu, Fe, Mn, Mo, or Zn between 'Nemaguard' and 'Rootpac 40' in response to salinity (Supplementary Fig. S3). However, 'Rootpac 40' had a small but significant decrease in leaf P accumulation. 'Nemaguard' maintained a similar leaf P accumulation under both control and salinity conditions (Supplementary Fig. S3c).

Transcript sequencing and gene expression. To understand the salinity tolerance mechanism at the transcriptome level of salt-tolerant 'Rootpac 40' and salt-sensitive 'Nemaguard' rootstocks, we performed a three-factor RNA-Seq experiment using two levels per factor to identify differential gene expression between the following variables: 1) treatment type (control *vs*. salt treatment); 2) rootstock (salt-sensitive, 'Nemaguard' *vs*. salt-tolerant, 'Rootpac 40'); and 3) tissue type (leaf *vs*. root). We named our experimental samples as CNL for Control 'Nemaguard' Leaf, TNL for Treatment 'Nemaguard' Leaf, CNR for Control 'Nemaguard' Root, TNR for Treatment 'Nemaguard' Root, CRL for Control 'Rootpac 40' Leaf, TRL for Treatment 'Rootpac 40' Leaf, CRR for Control 'Rootpac 40' Root, and TRR for Treatment 'Rootpac 40' Root (Supplementary Table S1). Accordingly, we performed RNA sequencing for 24 samples that included

three biological replicates of leaf and root tissues harvested from 'Rootpac 40' and 'Nemaguard' rootstocks. We observed a total of 1,586,189,238 raw reads for 24 libraries with an average of 66,091,218 raw reads/library (Supplementary Table S2). After removing adapter sequences, low-quality reads, and ambiguous nucleotides, we obtained 1,551,884,576 clean reads, consisting of 233 gigabases (Gb) with an average of 9.7 Gb per library (Supplementary Table S2).

To analyze differential gene expression, RNA-Seq reads from each sample were aligned to the annotated *Prunus persica* genome, which produced an average mapping of 92.27% for individual samples (Supplementary Table S2). The genome sequencing of *P. persica* predicted 27,852 protein-coding genes[26]. Our analyses identified 14,985 DEGs in at least one of the comparisons: Treatment *vs.* control, 'Nemaguard' *vs.* 'Rootpac 40', or Leaf *vs.* Root (Fig. 2 and Table 2). Gene expression-based cluster analysis identified two main groups based on tissue types, one for root tissues and the other for leaf tissues (Fig. 2a). Genes from CRR and TRR formed one subgroup, and genes from CNR and TNR formed the other subgroup within the root and leaf groups (Fig. 2a).

Table 2
Differentially Expressed Genes (DEGs) identified in different comparisons.

Comparison	Groups	DEGs	Upregulated	Downregulated
Salt *vs.* Control	TNL *vs.* CNL	61	4	57
	TNR *vs.* CNR	48	30	18
	TRL *vs.* CRL	9	1	8
	TRR *vs.* CRR	7	1	6
CNL *vs.* CRL	3403	1338	2065	
CNR *vs.* CRR	1347	542	805	
TNL *vs.* TRL	2064	799	1265	
TNR *vs.* TRR	1559	706	853	
Leaf *vs.* Root	CNL *vs.* CNR	7853	3456	4377
	CRL *vs.* CRR	6725	3211	3514
	TNL *vs.* TNR	7913	3231	4682
	TRL *vs.* TRR	7220	3267	3953

CNL, control 'Nemaguard' leaf; TNL, treated 'Nemaguard' leaf; CNR, control 'Nemaguard' root, TNR, treated 'Nemaguard' root; CRL, control 'Rootpac 40' leaf, TRL, treated 'Rootpac 40' leaf; CRR, control 'Rootpac 40' root; TRR, treated 'Rootpac 40' root

Gene expression analyses were performed to identify DEGs in three different comparisons (treatment *vs.* control; salt-sensitive rootstock *vs.* salt-tolerant rootstock; and leaf *vs.* root) (Fig. 2, Table 2 and Supplementary Table S3). For the treatment *vs.* control comparisons, 122 DEGs were identified, including 61 for TNL *vs.* CNL (4 upregulated and 57 downregulated), 48 for TNR *vs.* CNR (30 upregulated and 18 downregulated), 9 for TRL *vs.* CRL (1 upregulated and 8 downregulated), and 7 for TRR *vs.* CRR (1 upregulated and 6 downregulated) (Fig. 2b, Table 2 and Supplementary Table S3). For the comparisons between salt-sensitive ('Nemaguard') *vs.* salt-tolerant ('Rootpac 40') rootstocks, 4,765 DEGs were identified, including 3,403 for CNL *vs.* CRL (1,338 upregulated and 2,065 downregulated), 1,347 for CNR *vs.* CRR (542 upregulated and 805 downregulated), 2,064 for TNL *vs.* TRL (799 upregulated and 1265 downregulated), and 1,559 for TNR *vs.* TRR (706 upregulated and 853 downregulated) (Fig. 2c, Table 2 and Supplementary Table S3). For the comparisons between leaf *vs.* root, 10,098 DEGs were identified, including 7,833 in CNL *vs.* CNR (3,456 upregulated and 4,377 downregulated), 6725 in CRL *vs.* CRR (3,211 upregulated and 3,514 downregulated), 7, 913 in TNL *vs.* TNR (3231 upregulated and 4682 downregulated) 7,220 in TRL *vs.* TRR (3,267 upregulated and 3,953 downregulated) (Fig. 2d, Table 2 and Supplementary Table S3).

Verification of DEGs using qRT-PCR. To validate RNA-Seq data, we randomly selected a total of 41 DEGs (18 upregulated and 23 downregulated genes) from different comparison groups to perform qRT-PCR (Supplementary Tables S4 & S5). Among the 41 DEGs, 33 genes were evaluated for single comparisons, and four genes were evaluated for two different comparisons. Relative normalized expressions data were compared for three genes for CNL *vs.* TNL; four genes for CNR *vs.* TNR; four genes for CRL *vs.* TRL; one gene for CRR *vs.* TRR; seven genes for CNL *vs.* CRL; eight genes for CNR *vs.* CRR; six genes for TNL *vs.* TRL; and eight genes for TNR *vs.* TRR (Fig. 3). For most genes, qRT-PCR assay results showed a general trend of expression profiles observed in the RNA-Seq experiment, confirming the validity of the RNA-Seq results (Fig. 3 & Supplementary Fig. S4). For example, *Prupe.8G148400*, which encodes a serine carboxypeptidase showed 8.9- and 10.3-fold upregulation in CRL compared to CNL, in RNA-Seq and qRT-PCR, respectively. Still, a few genes did not exhibit a similar fold change in qRT-PCR compared to RNA-Seq results. For example, *Prupe.1G476500*, which encodes a BURP protein, showed 95.3- and 42.3-fold upregulation in CNL compared to CRL, in RNA-seq and qRT-PCR, respectively. Although expression levels differed between RNA-Seq and qRT-PCR results for a few genes, overall trends (downregulation or upregulation) were the same.

Gene ontology (GO) enrichment analysis of DEGs. To study functional enrichment analysis of DEGs in treatment *vs.* control and 'Nemaguard' *vs.* 'Rootpac 40', we performed GO enrichment analysis primarily for three major categories: molecular function, MF; cellular component, CC; and biological processes, BP (Supplementary Table S6). In treatment vs. control comparisons, 111, 86, 20, and 31 GO terms were enriched in TNL *vs.* CNL, TNR *vs.* CNR, TRL *vs.* CRL, and TRR *vs.* CRR, respectively (Supplementary Table S6). In 'Nemaguard' *vs.* 'Rootpac 40' comparison, 1552, 901, 1145, and 931 GO terms were enriched in CNL *vs.* CRL, CNR *vs.* CRR, TNL *vs.* TRL, and TNR *vs.* TRR, respectively (Supplementary Table S6).

KEGG Enrichment Analysis of DEGs. To find out which biological pathways were enriched in treatment *vs.* control and 'Nemaguard' (salt-sensitive) *vs.* 'Rootpac 40' (salt-tolerant), KEGG enrichment analysis of DEGs was performed for each pairwise comparison. In salt treatment *vs.* control comparisons, 1, 4, 0, and 1 number of pathway(s) were enriched in TNL *vs.* CNL, TNR *vs.* CNR, TRL *vs.* CRL, and TRR *vs.* CRR, respectively (Supplementary Table S7). In salt-sensitive ('Nemaguard') *vs.* salt-tolerant ('Rootpac 40') comparisons, 7, 5, 3, and 4 pathways were enriched in CNL *vs.* CRL, CNR *vs.* CRR, TNL *vs.* TRL, and TNR *vs.* TRR, respectively (Supplementary Table S7).

DEGs associated with stress pathways. Multiple pathways regulate salt stress signaling in plants. Therefore, all identified DEGs were analyzed to determine their association with primary stress pathways such as phytohormone signaling, redox signaling, and calcium signaling (Fig. 4 and Supplementary Tables S8, S9, S10).

***Hormonal Signaling*.** In treatment *vs.* control comparisons, two DEGs were upregulated, 1 for jasmonic acid (JA) and 1 for salicylic acid (SA) in TNL *vs.* CNL (Fig. 4 and Supplementary Table S8). In TNR *vs.* CNR, 5 DEGs were associated with hormonal signaling, 2 DEGs (one upregulated and one downregulated) for indole acetic acid (IAA), 1 downregulated DEG for JA, and 2 downregulated DEGs were for SA. No DEGs were identified for hormonal signaling in two comparisons: TRL *vs.* CRL and TRR *vs.* CRR (Fig. 4 and Supplementary Table S8). In salt-sensitive *vs.* salt-tolerant comparisons, 117, 26, 59, and 37 DEGs associated with hormone signaling were identified for the CNL *vs.* CRL, CNR *vs.* CRR, TNL *vs.* TRL, and TNR *vs.* TRR comparisons, respectively (Fig. 4a and Supplementary Table S8). The highest number of DEGs involved in hormonal signaling were identified for IAA, followed by SA and ABA.

***Redox signaling*.** In treatment *vs.* control comparisons, 4 DEGs associated with redox signaling were downregulated in TNL *vs.* CNL; of these, 3 DEGs were for heme, and 1 DEG was for glutathione (GSH) (Fig. 4b and Supplementary Table S9). Three DEGs (1 upregulated and two downregulated) were involved in redox signaling, specifically associated with heme in TNR *vs.* CNR. No DEGs associated with redox signaling were identified for TRL *vs.* CRL and TRR *vs.* CRR comparisons (Fig. 4b and Supplementary Table S9). In salt-sensitive *vs.* salt-tolerant comparisons, 123, 64, 52, and 76 DEGs regulating redox pathways were identified for the CNL *vs.* CRL, TNL *vs.* TRL, CNR *vs.* CRR, TNR *vs.* TRR comparisons, respectively (Fig. 4b and Supplementary Table S9). The highest number of DEGs associated with redox signaling were identified for heme, followed by GSH.

Calcium signaling. In the salt treatment *vs.* control comparisons, one DEG was downregulated in TNL *vs.* CNL, and one DEG was upregulated in TNR *vs.* CNR (Fig. 4c and Supplementary Table S10). No DEGs were involved in calcium signaling in the TRL *vs.* CRL and TRR *vs.* CRR comparisons (Fig. 4c and Supplementary Table S10). In salt-sensitive *vs.* salt-tolerant comparisons, 40, 27, 10, and 14 DEGs involved in calcium signaling were identified for the CNL *vs.* CRL, TNL *vs.* TRL, CNR *vs.* CRR, TNR *vs.* TRR comparisons, respectively (Fig. 4c and Supplementary Table S10).

DEGs associated with transporters. Transporters play critical roles in ion distribution and homeostasis in plants. Our observations indicated that the salinity tolerance differences between 'Rootpac 40' and

‘Nemaguard’ were primarily due to contrasting accumulation of Na, Cl, and K. This prompted us to analyze DEGs that encode transporters. Our analysis identified a total of 1,194 transporter DEGs in treatment *vs.* control comparisons and salt-sensitive *vs.* salt-tolerant comparisons (Fig. 5 and Supplementary Table S11).

In TNL *vs.* CNL comparison, 8 DEGs were found encoding 7 families of transporters, including the ATP-binding cassette (ABC) superfamily, the divalent anion Na^+ symporter (DASS) family, and the intracellular chloride channel (CLIC) family. In TNR *vs.* CNR, 6 DEGs were identified, encoding 6 families of transporters, including the ATP-binding cassette (ABC) superfamily and the autotransporter-1 (AT-1) family (Fig. 5 and Supplementary Table S11). No DEGs were identified encoding transporter families in TRL *vs.* CRL and TRR *vs.* CRR comparisons. In salt-sensitive *vs.* salt-tolerant comparisons, 488 DEGs were found encoding 76 transporter families in CNL *vs.* CRL, including the intracellular chloride channel (CLIC) family, the voltage-gated ion channel (VIC) superfamily, and the monovalent cation:proton antiporter-1 (CPA1) family. For TNL *vs.* TRL, 319 DEGs were found encoding 63 families of transporters, including the polycystin cation channel (PCC) family, the cation channel-forming heat shock protein-70 (Hsp70) family, the Glycoside-Pentoside-Hexuronide (GPH): cation symporter family, the calcium-dependent chloride channel (Ca-ClC) family and the K^+ uptake permease (KUP) family. In CNR *vs.* CRR, 170 DEGs encoded 54 transporter families, including the voltage-gated K^+ channel ÃŽÂ²-subunit (KvÃŽÂ²) family, the anion exchanger (AE) family, and the proton-dependent oligopeptide transporter (POT/PTR) family. In TNR *vs.* TRR, 203 DEGs encoded 58 transporter families, including the DASS family and the autotransporter-1 (AT-1) family (Fig. 5 and Supplementary Table S11). Our analyses also revealed that DEGs encoding similar transporters across comparisons (Fig. 5 and Supplementary Table S11).

Discussion

The goals of this study were to examine the morphological, biochemical, and physiological mechanisms of salinity tolerance of ‘Rootpac 40’ and ‘Nemaguard’ rootstocks and to identify links to underlying genetic factors through transcriptome analyses. We compared the rootstocks ‘Rootpac 40’ with ‘Nemaguard’ under control and salinity conditions for relative survival rate, relative growth rate (specifically trunk diameter), leaf ion concentration, accumulation of proline, antioxidant capacity, phenol H accumulation, chlorophyll content, net photosynthesis, stomatal conductance, and global gene expression by performing RNA-Seq analysis.

The comparison of ‘Rootpac 40’ and ‘Nemaguard’ for various parameters established a relatively higher salinity tolerance of ‘Rootpac 40’ compared to ‘Nemaguard’. First, in response to salinity treatment, ‘Rootpac 40’ showed more than 90% relative survival rate whereas ‘Nemaguard’ showed only 38.9% relative survival rate (Fig. 1a); and in response to salinity treatment, ‘Rootpac 40’ showed better growth than ‘Nemaguard’ as determined by the relative change in trunk diameter (Fig. 1b). Second, ‘Rootpac 40’ rootstock accumulated eight-fold less Na compared to Nemagurd in leaf tissue (Fig. 1d), indicating that ‘Rootpac 40’ has the better ability to control Na accumulation in leaf during salinity stress. Third, ‘Rootpac 40’ showed 1.75-fold less Cl accumulation than ‘Nemaguard’ in response to salinity treatment indicating

that ‘Rootpac 40’ may take less Cl from soil and/or possess better Cl^- exclusion machinery (Fig. 1e). Fourth, ‘Rootpac 40’ showed a higher accumulation of K in response to salinity treatment than the control, whereas ‘Nemaguard’ showed a reduced accumulation of K in response to salinity treatment than control (Fig. 1f); treatment/control (T/C) values for K accumulation were 1.14 and 0.75 for ‘Rootpac 40’ and ‘Nemaguard’, respectively (Fig. 1f). Finally, the K/Na value was more than 10 for ‘Rootpac 40’ and was 0.75 for ‘Nemaguard’ (data not shown). Based on several different parameters analyzed, ‘Rootpac 40’ is a salt-tolerant, and ‘Nemaguard’ is a salt-sensitive rootstock. In a previous study, screening of 14 almond rootstocks with different genetic backgrounds revealed that peach-almond hybrids (‘such as Rootpac 40’) have better salinity tolerance than peach-based rootstocks (such as ‘Nemaguard’)[21].

To find out differences in gene expression in response to salinity stress at the transcriptome level, an RNA-Seq experiment was performed on root and leaf tissues of ‘Nemaguard’ (salt-sensitive) and ‘Rootpac 40’ (salt-tolerant), under the control and salinity treatments (Supplementary Table S1). Gene clustering analysis revealed that the highest number of DEGs for leaf *vs.* root comparisons (10,098), followed by salt-sensitive *vs.* salt-tolerant comparisons (3,403 DEGs), and in treatment *vs.* control comparisons (122 DEGs) (Fig. 2). A higher number of DEGs were detected in salt-sensitive *vs.* salt-tolerant comparisons than treatment *vs.* control comparisons, suggesting that genotype-specific differences are more critical in *Prunus* than treatment-specific differences.

Phytohormones are important signaling components and play critical roles in response to various stresses, including salinity stress[27,28]. Expectedly, a higher number of genes associated with phytohormone signaling were differentially expressed in salt-sensitive *vs.* salt-tolerant genotype comparisons than in treatment *vs.* control comparisons (Fig. 4a & Supplementary Table S8). Our analysis revealed the highest number of DEGs associated with auxin (IAA), followed by SA, and ABA; only a few DEGs were associated with GA, JA, BRs, cytokinin, or ethylene (Fig. 4a & Supplementary Table S8). These observations indicate that auxin, SA, and ABA may play critical signaling roles in response to salinity stress in *Prunus*. Additionally, in salt-sensitive *vs.* salt-tolerant comparisons, a significantly higher number of DEGs were observed in leaves than roots, suggesting a more critical role of hormonal signaling in leaf during salinity stress[29].

Reactive oxygen species (ROS) function as essential secondary messengers in cellular signaling in responses to various stresses in plants. Over accumulation of ROS (hydrogen peroxide, hydroxyl radicals, and superoxide anions) negatively impacts the function of molecular machinery and cellular structures, and uncontrolled over-accumulation of ROS could lead to cell death[30]. To maintain a non-toxic level of ROS, plants have both non-enzymatic and enzymatic antioxidative systems, which also play important roles in abiotic stress tolerance. Plants have many ROS scavenging enzymes, including glutathione S-transferase, superoxide dismutase, ascorbate peroxidase (APX), monodehydroascorbate reductase, dehydroascorbate reductase, glutathione reductase, peroxiredoxin, and catalase[31]. Plants also produce non-enzymatic antioxidants, including glutathione (GSH), phenolic compounds, tocopherols, and ascorbic acid. In plants, heme-containing proteins like catalase and APX play critical roles in ROS homeostasis[32].

For redox signaling, we identified the highest number of DEGs encoding heme-containing proteins, suggesting critical roles of these proteins in salinity tolerance (Fig. 4b and Supplementary Table S9). Additionally, genes associated with glutathione (GSH), ascorbate, and catalase were also differentially regulated, indicating their roles in ROS homeostasis in response to salinity stress in *Prunus* (Fig. 4b and Supplementary Table S9).

Calcium serves as an important second messenger in cellular signaling, including salinity stress-induced response[33]. In treatment *vs*. control comparisons, only 2 DEGs associated with calcium signaling were identified in 'Nemaguard' (Fig. 4c). Nevertheless, in 'Rootpac 40' no DEGs were identified associated with calcium signaling. These findings suggest that the expressions of genes associated with calcium signaling are stable under the control and the salinity treatments for both rootstocks. In contrast, more than 90 DEGs were identified in salt-sensitive *vs*. salt-tolerant comparisons, indicating that the expression differences in Ca^{2+} signaling genes between two genotypes may explain differences in their salinity tolerance (Fig. 4c).

Calcium signaling plays a key role in salinity tolerance in plants by activating the SOS signaling pathway, which is critical for Na homeostasis[34,35]. In addition to SOS3 (aka CBL4), CBL10 serves as a calcium sensor during salinity stress[36]. Salinity stress induces intracellular Ca^{2+} concentration; upon sensing Ca^{2+}, CBL10 interacts and activates SOS2 (aka CIPK24). Subsequently, SOS2 phosphorylates SOS1 that in turn activates SOS1. Active SOS1 extrudes Na^{+} from the inside of the cell to the outside. *Prupe.1G412900* encodes CBL10, which showed much higher expression in leaf and root tissues of 'Rootpac 40' than 'Nemaguard' irrespective of salinity treatment status (both in control and saline treatment conditions) (Supplementary Table S3). The higher expression of CBL10 in 'Rootpac 40' may be critical in maintaining Na^{+} homeostasis, providing higher salinity tolerance compared to 'Nemaguard'.

In addition to plant growth and development, potassium homeostasis is vital for salinity tolerance. In response to salinity, we observed an increased leaf K accumulation in 'Rootpac 40' but decreased in 'Nemaguard' (Fig. 2). Potassium channels and transporters play essential roles in K^{+} absorption from the soil. AKT1 (Arabidopsis K^{+} transporter 1) plays an essential role in K^{+} uptake from soil[37]. Our analyses identified a low expression of *AKT1* (*Prupe.1G472600*) in control 'Nemaguard' leaf (CNL) compared to the control 'Rootpac 40' leaf (CRL) (Supplementary Table S3). Similarly, we also observed a higher expression of *AKT1* in TRL compared to TNL. Additionally, higher expression of *AKT1* was observed in TRR compared to TNR. These facts suggest that higher expression of *AKT1* may have contributed to a higher concentration of K during control and salinity treatment condition in 'Rootpac 40'. Hence, *AKT1* may be a determinant for salinity tolerance in *Prunus*. Similarly, both under control and treatment conditions (CNL *vs.* CRL and TNL *vs.* TRL), lower expression of *Prupe.5G236500* was observed, which encodes a potassium transporter. Arabidopsis *KUP8* (potassium uptake permease 8) is an ortholog *Prupe.5G236500*. In Arabidopsis, 13 genes, including *KUP8*, belong to the K^{+} uptake family (KUP/HAK/KT), are implicated in potassium transport and translocation[38]. Therefore, higher expression

of *Prupe.5G236500* in ‘Rootpac 40’ leaf compared to ‘Nemaguard’ in control and salinity treatment conditions may have contributed to higher accumulation of K^+ in ‘Rootpac 40’.

We observed a lower accumulation of Cl in ‘Rootpac 40’ compared to ‘Nemaguard’ in response to salinity stress. Our differential gene expression analysis identified a few promising candidate genes. For example, *Prupe.3G053200* encodes anoctamin-10 (ANO10)/ chloride channel. Lower expression of this gene was observed in CNL compared to CRL (Supplementary Table S3). Similarly, lower expression of this gene was in TNL compared to TRL. Arabidopsis ortholog of this gene, *AtTMEM16*, is an anion/H^+ symporter that prefers Cl^- over NO_3^-, suggesting that *Prupe.3G053200* may have contributed to differential accumulation of Cl in both rootstocks in response to salinity[39]. Functional characterization of *Prupe.3G053200* should reveal its biological role in Cl^- homeostasis in response to salinity. Additionally, *Prupe.7G202700*, which encodes a mechanosensitive ion channel, was found to have lower expression in TNL compared to TRL (Supplementary Table S3), which might have contributed to lower accumulation of Cl in ‘Rootpac 40’ compared to ‘Nemaguard’ as it can extrude Cl^- from inside the cell to outside[40].

A plant's ability to tolerate salt has been linked with total phenolics and antioxidant capacity[12,41]. In the present study, neither ‘Rootpac 40’ nor ‘Nemaguard’ showed significant differences between control and salinity for total phenolics or the antioxidant capacity resulting from the ORAC test, suggesting that the salinity tolerance of these rootstocks was not directly dependent on total phenolics or antioxidant capacity measured in terms of relative survival rate or leaf ion accumulation precisely for Na and Cl (Fig. 1).

Our findings revealed that ‘Nemaguard’ (salt-sensitive) showed significant induction of proline accumulation in response to salinity, whereas ‘Rootpac 40’ (salt-tolerant) did not (Fig. 1C). Higher proline accumulation in the salt-sensitive rootstock may indicate that ‘Nemaguard’, but not ‘Rootpac 40’, was under an increased stress level resulting from the applied salinity of EC_w = 3.0 dS m^{-1}. Accordingly, a previous comparative analysis between 14 almond rootstocks revealed that in response to 10-month salinity treatment, rootstocks that accumulated less proline were more salt-tolerant than rootstocks that accumulated higher proline[21]. Also, the same report described that the treatment/control (T/C) ratio of proline accumulation had an inverse correlation with survival rate and positive correlation for Na or Cl accumulation in leaf and higher salinity tolerance ability[21], which agrees with the proline salt-response values observed in the present study (Fig. 1). These facts suggest that the amount of proline accumulation in *Prunus* genotypes depends on the amount of stress they sense. Under saline conditions, salt-sensitive genotypes are under higher stress than salt-tolerant genotypes; hence they accumulate more proline. It has also been suggested that proline accumulation is an indicator of salinity stress in real agricultural settings[21].

In addition to the different mechanisms discussed above, our analysis identified several candidate genes that also showed extreme differences between salinity treatment *vs.* control and ‘Nemaguard’ *vs.* ‘Rootpac 40’. For instance, higher expression of aquaporin *PIP1-2* (*Prupe.5G101400*) was observed in

TRR compared to TNR, suggesting that it may be critical for salinity tolerance in *Prunus* (Supplementary Table S3). Aquaporins are known to play positive roles in salinity tolerance in other plant species[42]. A recent report indicates that overexpression of lotus *PIP1-2* (*NnPIP1-2*) in Arabidopsis provides salinity tolerance[43]. NPR4 has been shown to play a negative regulatory role in salinity tolerance[44]. *Prupe.2G080900*, which encodes an ankyrin repeat-containing protein NPR4, was differentially expressed in TNL *vs.* CNL and TRL *vs.* CRL comparisons with a $\log_2$ fold change value of 6.6 and − 6.3, respectively (Supplementary Table S3). These findings propose that upregulation of NPR4 in 'Nemaguard' leaf and downregulation in root in response to salinity contributed toward the salt sensitivity of 'Nemaguard' compared to 'Rootpac 40'. F-box protein has been shown to act as a negative regulator in response to salinity tolerance[45]. *Prupe.1G273900* encodes for an F-box protein showed higher expression ($\log_2$ fold change value of 12.6) in TNR compared to TRR, indicating that upregulation of *Prupe.1G273900* may have contributed negatively toward salinity tolerance in 'Nemaguard'. Berberine bridge enzyme, betaglucosidase, and MLP like protein are known to contribute to salinity tolerance[46–48]. *Prupe.4G097000*, *Prupe.6G136700*, and *Prupe.1G327700*, which encode berberine bridge enzyme, betaglucosidase, and MLP like protein, respectively, were downregulated in response to salinity in 'Nemaguard' leaves compared to control (TNL *vs.* CNL) with $\log_2$ fold change values of -9.2, -8.6, and − 8.3. These observations suggest that downregulation of these three genes under salinity compared to control negatively impacted salinity tolerance in 'Nemaguard' (Supplementary Table S3). In TRL *vs.* CRL comparison, *Prupe.1G032800* ($\log_2$ fold change value of 14.6), which encodes berberine bridge enzyme, was upregulated under salinity compared to control, suggesting that this gene positively contributes to salinity tolerance in 'Rootpac 40'. GDSL esterase/lipase LTL1 is a positive regulator of salinity tolerance in Arabidopsis[49]. In response to salinity, LTL1 encoded by *Prupe.6G354100* was downregulated both in 'Nemaguard' leaves ($\log_2$ fold change value of -33) and roots ($\log_2$ fold change value of -27) compared to 'Rootpac 40' (TNL *vs.* TRL & TNR *vs.* TRR comparisons). Additionally, under control condition, lower expression of this gene was observed in 'Nemaguard' leaves compared to 'Rootpac 40' leaves (CNL vs. CRL) ($\log_2$ fold change value of -26). These facts indicate that downregulation of *Prupe.6G354100* in 'Nemaguard' compared to 'Rootpac 40' negatively affected salinity tolerance in 'Nemaguard'. Altogether, differential gene expression analysis revealed that downregulation of genes that are positive regulators and upregulation of genes that are negative regulators of salinity tolerance contributed to the lower salinity tolerance of 'Nemaguard', and the opposite expressions contributed to the higher salinity tolerance in 'Rootpac 40'.

Materials And Methods

Plant material and salt treatment. All experiments were performed at the United States Salinity Laboratory (USDA-ARS) in Riverside, CA. 'Nemaguard' and 'Rootpac 40' plants were obtained from Burchell and Agromillora nurseries, respectively, and transplanted into 6 L pots containing 1:1 sandy loam soil: sand. The experiment was conducted in a randomized complete block design with both rootstocks, three plants per replication (each pot containing one plant), three replications for control and saline water treatment.

The compositions of both control and saline treatments are indicated in Table 1. Riverside city water was used as control, and saline water contained various salts representing natural saline water composition. NPK nutrients concentrations were the same for control and treatment water. The electrical conductivity (EC_w) of control irrigation was 1.36 dS $m^{-1,}$ and the EC_w for treatment saline irrigation was 3.0 dS m^{-1}. The pH of both control and treatments was maintained between 7.3 and 7.6. Every other day, 600 ml of control or saline water was applied to each plant. All plants were treated for 10 months.

To study gene expression at the transcriptome level, approximately one-year-old 'Nemaguard' and 'Rootpac 40' rootstocks were irrigated with Riverside city water for control and high saline water dominant in sodium chloride for treatment with mineral composition presented in Table 1. Subsequently, 48 hours after salinity treatment, roots and leaves were collected from three biological replicates (one plant/biological replicate) for RNA isolation.

Trunk diameter measurement, survival rate, and leaf ion analysis. Before the beginning of the experiment, a vernier caliper was used to measure the trunk diameter of all plants 10 cm above the soil level. At the end of treatment, final trunk diameter data collected to calculate relative change. After completion of treatment, the survival rate of 'Nemaguard' and 'Rootpac 40' data were collected. After eight weeks of treatment, leaf samples were collected for ion analysis. Tissue samples were dried in an oven. Subsequently, a Milestone Ethos E.Z. microwave was used for the digestion of the dried leaf samples. Macro- and micronutrient elements were analyzed using Perkin Elmer Optima ICP OES. Labconco chloridometer was used for chloride content analysis.

Physiological and biochemical analysis. Measurement of stomatal conductance and photosynthetic parameters were performed using Li-Cor 6400 Photosynthesis System (Li-Cor Biosciences, Lincoln, NE, USA) after eight weeks from the starting day of salt treatment. The details about the measurement method have been described in a previous report[21]. Leaf harvest and measurement and analyses of proline, total phenolics, and hydrophilic antioxidant capacity were performed as described previously[21].

RNA extraction and transcript sequencing. TRIzol reagent (Invitrogen, Carlsbad, CA, USA) was used for total RNA isolation from leaf and root tissues. Subsequently, all RNA samples were treated with DNase I to remove any DNA contamination (Thermo Scientific, Waltham, MA, USA). The quality and quantity of all RNA samples were checked using Bioanalyzer (Agilent Technologies, USA) and Nanophotometer (IMPLEN, CA, USA). Purification of mRNA from total RNA was performed using Poly-T oligo-attached magnetic beads. NEBNext Ultra RNA library prep kit for Illumina (NEB) was used for construction sequencing libraries. Illumina HiSeq platform was employed for RNA sequencing and to generate 150 bp paired-end reads (Novogene Corp. Inc., Sacramento, CA). To obtain clean sequences, raw reads were subsequently trimmed and clipped of adaptors using Trimmomatic[50]. Clean reads were analyzed for quality scores, Q20 (error 1 in 100) and Q30 (error 1 in 1000), and GC contents were analyzed utilizing FASTQC (http://www.bioinformatics.babraham.ac.uk/projects/fastqc/). Reads deemed to be clean were then used for further analysis.

Transcriptome assembly mapping. Raw reads were stored in a left.fq.gz file and a right.fq.gz file. A shell script was written to quantify the pair-end reads using the mapping-based mode on Salmon [51]. The index was created using the *Prunus persica* NCBIv2.1[52] Transcriptome assembly. The "validatemappings" flag was set so that the more sensitive selective-alignment algorithm could be used[52]. The "gcBias" flag was also set to allow Salmon to correct for potential fragment-level guanine-cytosine content biases in the input data. Quantification files containing the read counts were then output with the .sf extension.

Differential Gene Expression Analysis. The biomaRt package[53,54] (2.42.0) was used to create a table of Ensembl gene ids for *P. persica*. Using the tximport package[55] (1.14.0), .sf files from Salmon were then imported and mapped to their corresponding Ensembl gene name. A matrix was created containing the sample name as the column, gene ID as the row, and the corresponding read counts as the observations. Genes with lower than 5 counts were filtered out of the data, as they would not be of much use in the analysis. Differential expression analysis was performed using DESeq2 (1.26.0)[56]. The package uses a model based on the negative binomial distribution to estimate variance-mean dependence of the gene count data[56]. Adjusted p-values (*q*-values) were generated using Benjamini and Hochberg's method to control the false discovery rate[56]. The significance cutoff was set to $\alpha = 0.05$. Genes with an adjusted p-value lower than 0.05 and a $\log_2$ fold change with an absolute value greater than 2 were deemed differentially expressed (DE). If a gene satisfied both *q*-value ≤ 0.05 and $|\log_2(\text{fold change})| \geq 2$, it was considered significantly differentially expressed.

Using the differentially expressed genes, Venn diagrams and heatmaps were constructed. The Venn diagrams were made using the "VennDiagram" package in R[57]. Heatmaps were generated using the "pheatmap" package in R (https://cran.r-project.org/web/packages/pheatmap/index.html). For clustering purposes, a Z-score transformation $\left(Z = \frac{x-\mu}{\sigma}\right)$ was performed on the matrix of pooled read counts for differentially expressed genes.

Gene ontology annotation and enrichment analysis of DEGs. Gene ontology (GO) analysis of the differentially expressed genes was done using the GOseq (1.38.0) package in R[58]. We assumed that, within a category, all genes have the same probability of being chosen. This allowed us to use the Wallenius non-central hypergeometric distribution to perform the GO enrichment test. First, an over-representation test was performed using the DE genes as the input set. Next, the over-representation of the DE genes was tested for using an adjusted p-value cutoff of $\alpha = 0.05$. The effect size calculation was then performed by taking the p-value and performing a negative 10-base log transformation.

KEGG enrichment analysis of DEGs. KEGG (Kyoto Encyclopedia of Genes and Genomes, http://www.kegg.jp/) consists of databases containing information regarding high-level functions and utilities in biological systems. KEGG pathway enrichment analysis was done using the ClusterProfiler (3.18.1) in R[59]. To perform the enrichment, DE genes needed to be converted from their ensemble id to their Entrez id equivalent. KEGG pathways in the DEGs were then compared to pathways associated with the entire genome background using the hypergeometric distribution and adjusted for a high FDR. KEGG

terms with an adjusted p-value less than 0.05 were deemed to be significantly enriched. The effect size calculation was then performed by taking the p-value and performing a negative 10-base log transformation.

Functional analysis and visualization. Keywords for specified paths were searched for in each comparison using the built-in “grep” R function. Genes containing specific keywords were colored depending on the value of their $\log_2$ fold change within the comparison. For example, genes with a $\log_2$ fold change greater than 0 were colored blue for upregulation, and genes with a $\log_2$ fold change less than 0 were colored red for downregulation.

Transporter analysis. Tables containing Transporter families were obtained from the Transporter Classification Database (https://tcdb.org/). Pfam IDs were used to map the genes to their associated families and superfamilies.

Quantitative reverse transcription PCR (qRT-PCR). Forty-one genes were selected randomly for qRT-PCR analysis to validate RNA-Seq data (Supplementary Tables S5 & S6). qRT-PCR assays were performed as described previously[29]. RNA samples that were used for RNA-Seq library preparation were also used for qRT-PCR analyses. To remove DNA contamination, RNA samples were treated with DNase I (New England Biolabs Inc., Ipswich, MA). The Bio-Rad CFX96 System (Bio-Rad Laboratories, Hercules, CA) was used to perform qRT-PCR using the iTaq Universal SYBR Green One-Step Kit. All qRT-PCR reactions were performed in a total volume of 10 µl containing 20 ng total RNA, 0.75 µM of each of the primers, 5 µl of 2 × one-step SYBR® Green Reaction mix, and 0.125 µl iScript™ Reverse Transcriptase. The qRT-PCR conditions used were: 50°C for 10 min, 95°C for 1 min, followed by 40 cycles of 95°C denaturation for 10 s, 57°C annealing for 30 s, and 68°C extension for 30 s. *PpUBQ10*, *PpRPII*, *PpTEF2* were used as the reference for the analyses. All assays were conducted using RNA from three biological replicates and two technical replicates. To check DEGs, the cycle threshold (CT) values of all tested genes were compared to the reference, and subsequently, the difference in expressions was calculated.

The use of plants in the present study complies with international, national and/or institutional guidelines.

Abbreviations

qRT-PCR, *quantitative reverse transcription PCR;* ORAC, oxygen radical absorbance capacity; SPAD, Soil Plant Analysis Development; EC, electrical conductivity

Declarations

Acknowledgments

This study was supported by the Almond Board of California (project # Hort26-Sandhu) and the United States Department of Agriculture-Agricultural Research Service, National Program 301: Plant Genetic

Resources, Genomics, and Genetic Improvement (project number 2036-13210-012-00-D). In addition, the authors thank Ms. Pangki Xiong for the ion analyses. The authors also acknowledge suggestions provided by Dr. Chaoyang Zhao for bioinformatics analyses. Finally, the authors are grateful to Burchell and Agromillora nurseries for providing 'Nemaguard' and 'Rootpac 40' rootstocks, respectively, for salinity tolerance evaluation.

Author contributions

DS, JF, DLS, and TS conceptualized, designed, and supervised the experiments; MP and AK evaluated the genotypes, isolated and purified RNA; BA and MP performed the validation experiment; CD, MD, BA, and MP performed statistical analyses. BA, CD, MD, MP, and DS, analyzed and interpreted the data; The manuscript was written jointly with contributions from all the authors. All authors have read and approved the manuscript.

Conflict of Interest Statement

The authors declare no competing financial or non-financial interests concerning the work described. The funders had no role in the design of the study; in the collection, analyses, or interpretation of data; in the writing of the manuscript, or in the decision to publish the results.

Supplemental Data

Supplementary material contains 11 supplementary Tables (Supplementary Tables S1 – S11) and 4 Supplementary Figures (Supplementary Fig. S1 – S4).

Data Availability Statement

Illumina HiSeq generated RNA-Seq reads are available in NCBI Sequence Read Archive (SRA) for the Bioproject: PRJNA732909 (https://www.ncbi.nlm.nih.gov/Traces/study/?acc=%20PRJNA732909&o=acc_s%3Aa). Additional datasets supporting this research are included in the paper and as supplementary materials.

References

1. Zhu, J. K. Plant salt tolerance. *Trends Plant Sci*, **6**, 66–71 https://doi.org/10.1016/s1360-1385(00)01838-0 (2001).
2. Welle, P. D. & Mauter, M. S. High-resolution model for estimating the economic and policy implications of agricultural soil salinization in California. *Environ. Res. Lett*, **12**, 094010 https://doi.org/10.1088/1748-9326/aa848e (2017).
3. Isayenkov, S. V. & Maathuis, F. J. M. Plant salinity stress: many unanswered questions remain. *Front. Plant Sci*, **10**, https://doi.org/10.3389/fpls.2019.00080 (2019).

4. Zörb, C., Geilfus, C. M. & Dietz, K. J. Salinity and crop yield. *Plant Biol. (Stuttg)*, **21 Suppl** (1), 31–38 https://doi.org/10.1111/plb.12884 (2019).
5. Butcher, K., Wick, A., Desutter, T., Chatterjee, A. & Harmon, J. Soil Salinity: a threat to global food security. *Agronomy J*, **108**, 2189–2200 https://doi.org/10.2134/agronj2016.06.0368 (2016).
6. Xiong, L., Schumaker, K. S. & Zhu, J. K. Cell signaling during cold, drought, and salt stress. *Plant Cell*, **14 Suppl**, S165–183 https://doi.org/10.1105/tpc.000596 (2002).
7. Qiu, Q. S., Barkla, B. J., Vera-Estrella, R., Zhu, J. K. & Schumaker, K. S. Na+/H+ exchange activity in the plasma membrane of Arabidopsis. *Plant Physiol*, **132**, 1041 https://doi.org/10.1104/pp.102.010421 (2003).
8. Shi, H., Lee, B. H., Wu, S. J. & Zhu, J. K. Overexpression of a plasma membrane Na+/H+ antiporter gene improves salt tolerance in Arabidopsis thaliana. *Nat. Biotechnol*, **21**, 81–85 https://doi.org/10.1038/nbt766 (2003).
9. van Zelm, E., Zhang, Y. & Testerink, C. Salt tolerance mechanisms of plants. *Annu. Rev. Plant Biol*, **71**, 403–433 https://doi.org/10.1146/annurev-arplant-050718-100005 (2020).
10. Møller, I. S. & Tester, M. Salinity tolerance of Arabidopsis: a good model for cereals? *Trends Plant Sci*, **12**, 534–540 https://doi.org/10.1016/j.tplants.2007.09.009 (2007).
11. Jha, D., Shirley, N., Tester, M. & Roy, S. J. Variation in salinity tolerance and shoot sodium accumulation in Arabidopsis ecotypes linked to differences in the natural expression levels of transporters involved in sodium transport. *Plant Cell Environ*, **33**, 793–804 https://doi.org/10.1111/j.1365-3040.2009.02105.x (2010).
12. Sandhu, D., Cornacchione, M. V., Ferreira, J. F. S. & Suarez, D. L. Variable salinity responses of 12 alfalfa genotypes and comparative expression analyses of salt-response genes. *Sci. Rep*, **7**, 42958 https://doi.org/10.1038/srep42958 (2017).
13. CDFA. California Agricultural Exports 2017-18. *California Agricultural Statistics Review*, 2017-*18*, 105–118 (2018). .
14. Kamil, A. & Chen, C. Y. Health benefits of almonds beyond cholesterol reduction. *J. Agric. Food. Chem*, **60**, 6694–6702 https://doi.org/10.1021/jf2044795 (2012).
15. Tan, S. Y. & Mattes, R. D. Appetitive, dietary and health effects of almonds consumed with meals or as snacks: a randomized, controlled trial. *Eur. J. Clin. Nutr*, **67**, 1205–1214 https://doi.org/10.1038/ejcn.2013.184 (2013).
16. Fulton, J., Norton, M. & Shilling, F. Water-indexed benefits and impacts of California almonds. *Ecol. Indic*, **96**, 711–717 https://doi.org/10.1016/j.ecolind.2017.12.063 (2019).
17. Sandhu, D. & Acharya, B. R. Mechanistic insight into the salt tolerance of almonds. *Progressive Crop Consultant*, **4**, 44–49 (2019).
18. Shao, Y. *et al.* Investigation of salt tolerance mechanisms across a root developmental gradient in almond rootstocks. *Front. Plant Sci*, **11**, https://doi.org/10.3389/fpls.2020.595055 (2021).

19. Ranjbarfordoei, A., Samson, R. & Van Damme, P. Photosynthesis performance in sweet almond [Prunus dulcis (Mill) D. Webb] exposed to supplemental UV-B radiation. *Photosynthetica*, **49**, 107 https://doi.org/10.1007/s11099-011-0017-z (2011).
20. Mass, E. V. & Hoffman, G. J. Crop salt tolerance—current assessment. *J. Irrig. Drain. Div. [ZDB]*, **103**, 711–717 https://doi.org/10.1061/JRCEA4.0001137 (1977).
21. Sandhu, D. *et al.* Linking diverse salinity responses of 14 almond rootstocks with physiological, biochemical, and genetic determinants. *Sci. Rep*, **10**, 21087 https://doi.org/10.1038/s41598-020-78036-4 (2020).
22. Micke, W. C. & Resources, U. C. D. A. N. Almond Production Manual. (University of California, Division of Agriculture and Natural Resources, 1996).
23. Kaundal, A., Sandhu, D., Duenas, M. & Ferreira, J. F. S. Expression of the high-affinity K+ transporter 1 (PpHKT1) gene from almond rootstock 'Nemaguard' improved salt tolerance of transgenic Arabidopsis. *PLOS ONE*, **14**, e0214473 https://doi.org/10.1371/journal.pone.0214473 (2019).
24. Ahmad, R. *et al.* Whole genome sequencing of peach (Prunus persica L.) for SNP identification and selection. *BMC Genomics*, **12**, 569 https://doi.org/10.1186/1471-2164-12-569 (2011).
25. Alisoltani, A. *et al.* Parallel consideration of SSRs and differentially expressed genes under abiotic stress for targeted development of functional markers in almond and related Prunus species. *Sci. Hortic*, **198**, 462–472 https://doi.org/10.1016/j.scienta.2015.10.020 (2016).
26. Verde, I. *et al.* The high-quality draft genome of peach (Prunus persica) identifies unique patterns of genetic diversity, domestication and genome evolution. *Nat. Genet*, **45**, 487–494 https://doi.org/10.1038/ng.2586 (2013).
27. Verma, V., Ravindran, P. & Kumar, P. P. Plant hormone-mediated regulation of stress responses. *BMC Plant Biol*, **16**, 86 https://doi.org/10.1186/s12870-016-0771-y (2016).
28. Zhao, C., Sandhu, D. & Ferreira, J. F. S. Transcript analysis of two spinach cultivars reveals the complexity of salt tolerance mechanisms. *ACS Agricultural Science & Technology*, **1**, 64–75 https://doi.org/10.1021/acsagscitech.0c00063 (2021).
29. Kaundal, R. *et al.* Transcriptional profiling of two contrasting genotypes uncovers molecular mechanisms underlying salt tolerance in alfalfa. *Sci. Rep*, **11**, 5210 https://doi.org/10.1038/s41598-021-84461-w (2021).
30. Gill, S. S. & Tuteja, N. Reactive oxygen species and antioxidant machinery in abiotic stress tolerance in crop plants. *Plant Physiol. Biochem*, **48**, 909–930 (2010).
31. You, J. & Chan, Z. ROS regulation during abiotic stress responses in crop plants. *Fronti.Plant Sci*, **6**, https://doi.org/10.3389/fpls.2015.01092 (2015).
32. Nadarajah, K. K. ROS homeostasis in abiotic stress tolerance in plants. *Int. J. Mol. Sci*, **21**, 5208 https://doi.org/10.3390/ijms21155208 (2020).
33. Lamers, J., van der Meer, T. & Testerink, C. How plants sense and respond to stressful environments. *Plant Physiol*, **182**, 1624–1635 https://doi.org/10.1104/pp.19.01464 (2020).

34. Zhu, J. K. Salt and drought stress signal transduction in plants. *Annu. Rev. Plant Biol*, **53**, 247–273 https://doi.org/10.1146/annurev.arplant.53.091401.143329 (2002).
35. Zhao, C., William, D. & Sandhu, D. Isolation and characterization of salt overly sensitive family genes in spinach. *Physiol. Plant*, https://doi.org/10.1111/ppl.13125 (2020).
36. Quan, R. *et al.* SCABP8/CBL10, a putative calcium sensor, interacts with the protein kinase SOS2 to protect Arabidopsis shoots from salt stress. *Plant Cell*, **19**, 1415–1431 https://doi.org/10.1105/tpc.106.042291 (2007).
37. Hirsch, R. E., Lewis, B. D., Spalding, E. P. & Sussman, M. R. A role for the AKT1 potassium channel in plant nutrition., **280**, 918–921 https://doi.org/10.1126/science.280.5365.918 (1998).
38. Ahn, S. J., Shin, R. & Schachtman, D. P. Expression of KT/KUP genes in Arabidopsis and the role of root hairs in K+ uptake. *Plant Physiol*, **134**, 1135–1145 https://doi.org/10.1104/pp.103.034660 (2004).
39. Domingos, P. *et al.* Molecular and electrophysiological characterization of anion transport in Arabidopsis thaliana pollen reveals regulatory roles for pH, Ca2+ and GABA. *New Phytol*, **223**, 1353–1371 https://doi.org/10.1111/nph.15863 (2019).
40. Maksaev, G. & Haswell, E. S. MscS-Like10 is a stretch-activated ion channel from *Arabidopsis thaliana* with a preference for anions. *Proc. Natl. Acad. Sci. U S A* **109**, 19015–19020, doi:10.1073/pnas.1213931109 (2012).
41. Boestfleisch, C. & Papenbrock, J. Changes in secondary metabolites in the halophytic putative crop species *Crithmum maritimum* L., *Triglochin maritima* L. and *Halimione portulacoides* (L.) Aellen as reaction to mild salinity. *PLOS ONE* **12**, e0176303, doi:10.1371/journal.pone.0176303 (2017).
42. Wang, X. *et al.* Overexpression of the Jojoba aquaporin gene, ScPIP1, enhances drought and salt tolerance in transgenic Arabidopsis. *Int. J. Mol. Sci*, **20**, 1–13 https://doi.org/10.3390/ijms20010153 (2019).
43. Ziyuan, L. *et al.* Molecular cloning and functional analysis of lotus salt-induced *NnDREB2C*, *NnPIP1-2* and *NnPIP2-1* in *Arabidopsis thaliana*. *Mol. Biol. Rep.* **47**, 497–506, doi:10.1007/s11033-019-05156-0 (2020).
44. Xu, Y. Q. *et al.* Characterization of NPR1 and NPR4 genes from mulberry (Morus multicaulis) and their roles in development and stress resistance. *Physiol. Plant*, **167**, 302–316 https://doi.org/10.1111/ppl.12889 (2019).
45. Yu, Y. *et al.* The soybean F-box protein GmFBX176 regulates ABA-mediated responses to drought and salt stress. *Environ. Exp. Bot*, **176**, 104056 https://doi.org/10.1016/j.envexpbot.2020.104056 (2020).
46. Daniel, B. *et al.* Structure of a berberine bridge enzyme-like enzyme with an active site specific to the plant family Brassicaceae. *PLOS ONE*, **11**, e0156892–e0156892 https://doi.org/10.1371/journal.pone.0156892 (2016).
47. Xu, Z. Y. *et al.* A vacuolar β-glucosidase homolog that possesses glucose-conjugated abscisic acid hydrolyzing activity plays an important role in osmotic stress responses in Arabidopsis. *Plant Cell*, **24**, 2184–2199 https://doi.org/10.1105/tpc.112.095935 (2012).

48. Chen, J. Y. & Dai, X. F. Cloning and characterization of the Gossypium hirsutum major latex protein gene and functional analysis in Arabidopsis thaliana., **231**, 861–873 https://doi.org/10.1007/s00425-009-1092-2 (2010).
49. Naranjo, M. A., Forment, J., Roldán, M., Serrano, R. & Vicente, O. Overexpression of Arabidopsis thaliana LTL1, a salt-induced gene encoding a GDSL-motif lipase, increases salt tolerance in yeast and transgenic plants. *Plant Cell Environ*, **29**, 1890–1900 https://doi.org/10.1111/j.1365-3040.2006.01565.x (2006).
50. Bolger, A. M., Lohse, M. & Usadel, B. Trimmomatic: a flexible trimmer for Illumina sequence data., **30**, 2114–2120 https://doi.org/10.1093/bioinformatics/btu170 (2014).
51. Patro, R., Duggal, G., Love, M. I., Irizarry, R. A. & Kingsford, C. Salmon provides fast and bias-aware quantification of transcript expression. *Nat. Methods*, **14**, 417–419 https://doi.org/10.1038/nmeth.4197 (2017).
52. Srivastava, A. *et al.* Alignment and mapping methodology influence transcript abundance estimation. *Genome Biol*, **21**, 239 https://doi.org/10.1186/s13059-020-02151-8 (2020).
53. Durinck, S., Spellman, P. T., Birney, E. & Huber, W. Mapping identifiers for the integration of genomic datasets with the R/Bioconductor package biomaRt. *Nat. Protoc*, **4**, 1184–1191 https://doi.org/10.1038/nprot.2009.97 (2009).
54. Durinck, S. *et al.* BioMart and Bioconductor: a powerful link between biological databases and microarray data analysis., **21**, 3439–3440 https://doi.org/10.1093/bioinformatics/bti525 (2005).
55. Soneson, C., Love, M. I. & Robinson, M. D. Differential analyses for RNA-seq: transcript-level estimates improve gene-level inferences. *F1000Res*, **4**, 1521 https://doi.org/10.12688/f1000research.7563.2 (2015).
56. Love, M. I., Huber, W. & Anders, S. Moderated estimation of fold change and dispersion for RNA-seq data with DESeq2. *Genome Biol*, **15**, 550 https://doi.org/10.1186/s13059-014-0550-8 (2014).
57. Chen, H. & Boutros, P. C. VennDiagram: a package for the generation of highly-customizable Venn and Euler diagrams in R. *BMC Bioinform*, **12**, 1–7 https://doi.org/10.1186/1471-2105-12-35 (2011).
58. Young, M. D., Wakefield, M. J., Smyth, G. K. & Oshlack, A. Gene ontology analysis for RNA-seq: accounting for selection bias. *Genome Biol*, **11**, R14 https://doi.org/10.1186/gb-2010-11-2-r14 (2010).
59. Yu, G., Wang, L. G., Han, Y. & He, Q. Y. clusterProfiler: an R package for comparing biological themes among gene clusters. *OMICS*, **16**, 284–287 https://doi.org/10.1089/omi.2011.0118 (2012).

Figures

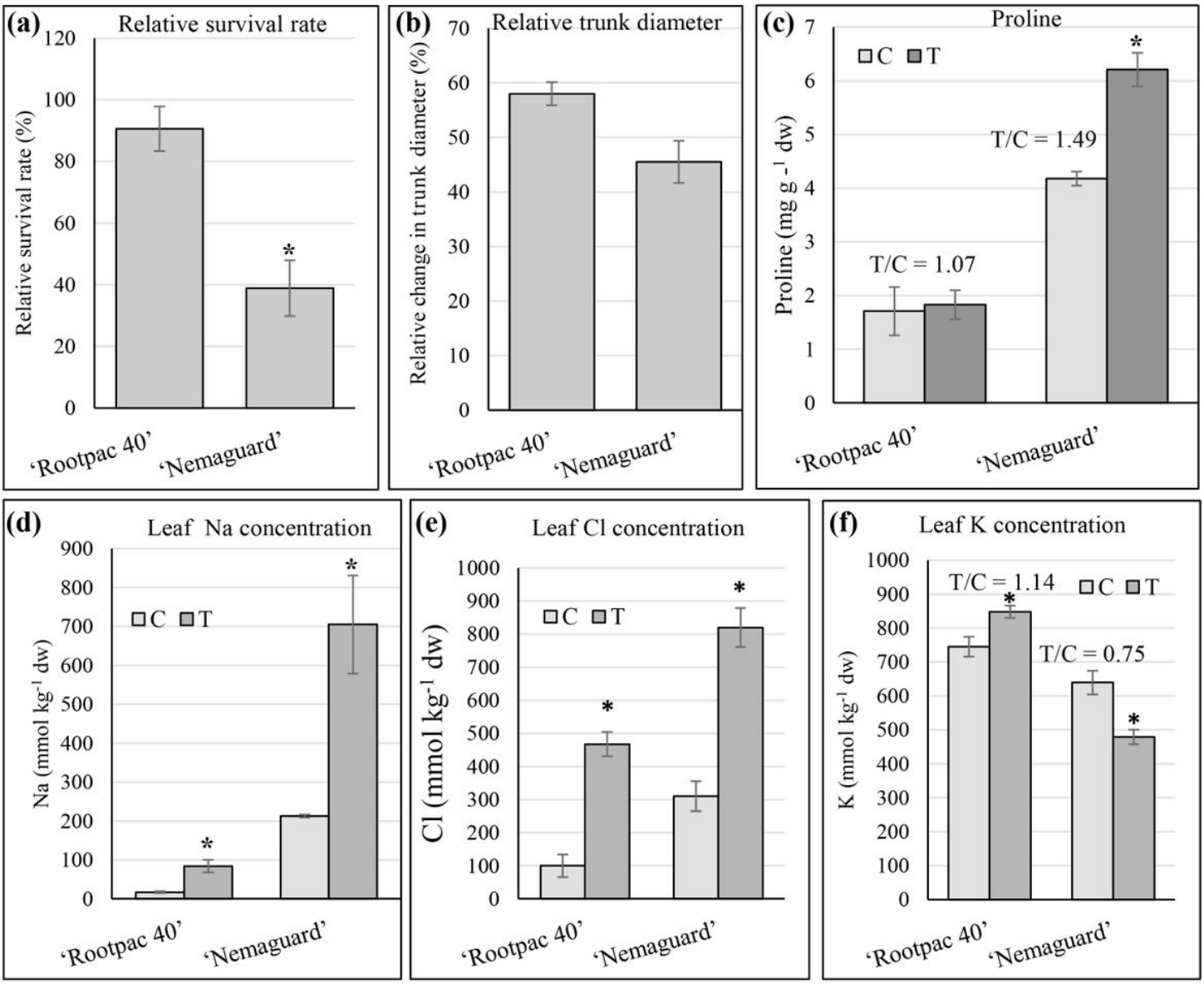

Figure 1

Performances of 'Rootpac 40' and 'Nemaguard' rootstocks under control and saline environments. (a) Relative survival rates (%) of 'Rootpac 40' and 'Nemaguard' rootstocks in response to the saline treatment compared to control. (b) Relative change in trunk diameters. (c) Leaf proline concentrations (d) Leaf Na concentrations. (e) Leaf Cl concentrations. (f) Leaf K concentrations. Error bars represent standard errors of three biological replicates. An asterisk (*) indicates a significant difference (t-test $p \leq 0.05$). C indicates control, and T indicates saline treatment.

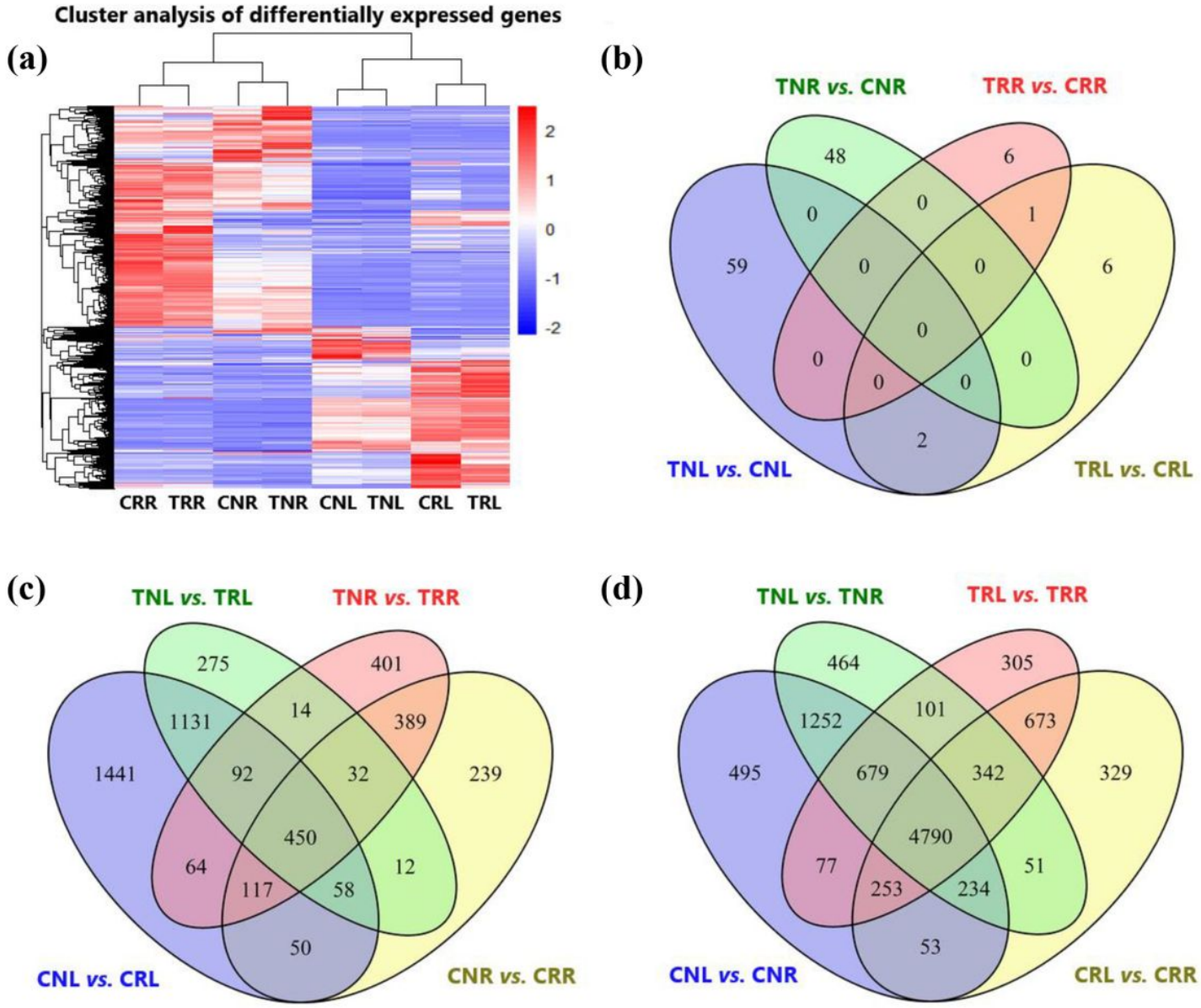

Figure 2

Heat map-based clustering and Venn diagram analysis of differentially expressed genes (DEGs). (a) Heatmap and hierarchical clustering DEGs across all eight samples. (b) Venn diagram shows the number of DEGs across four salt treatment vs. control comparisons. (c) Venn diagram shows the number of DEGs across four salt-sensitive ('Nemaguard') vs. four salt-tolerant ('Rootpac 40') comparisons. (d) Venn diagram shows the number of DEGs across four leaf vs. root comparisons. CNL, Control 'Nemaguard' Leaf; TNL, Treatment 'Nemaguard' Leaf; CNR, Control 'Nemaguard' Root; TNR, Treatment 'Nemaguard' Root; CRL, Control 'Rootpac 40' Leaf; TRL, Treatment Rootpac Leaf; CRR: control 'Rootpac 40' root; TRR, treatment 'Rootpac 40' Root

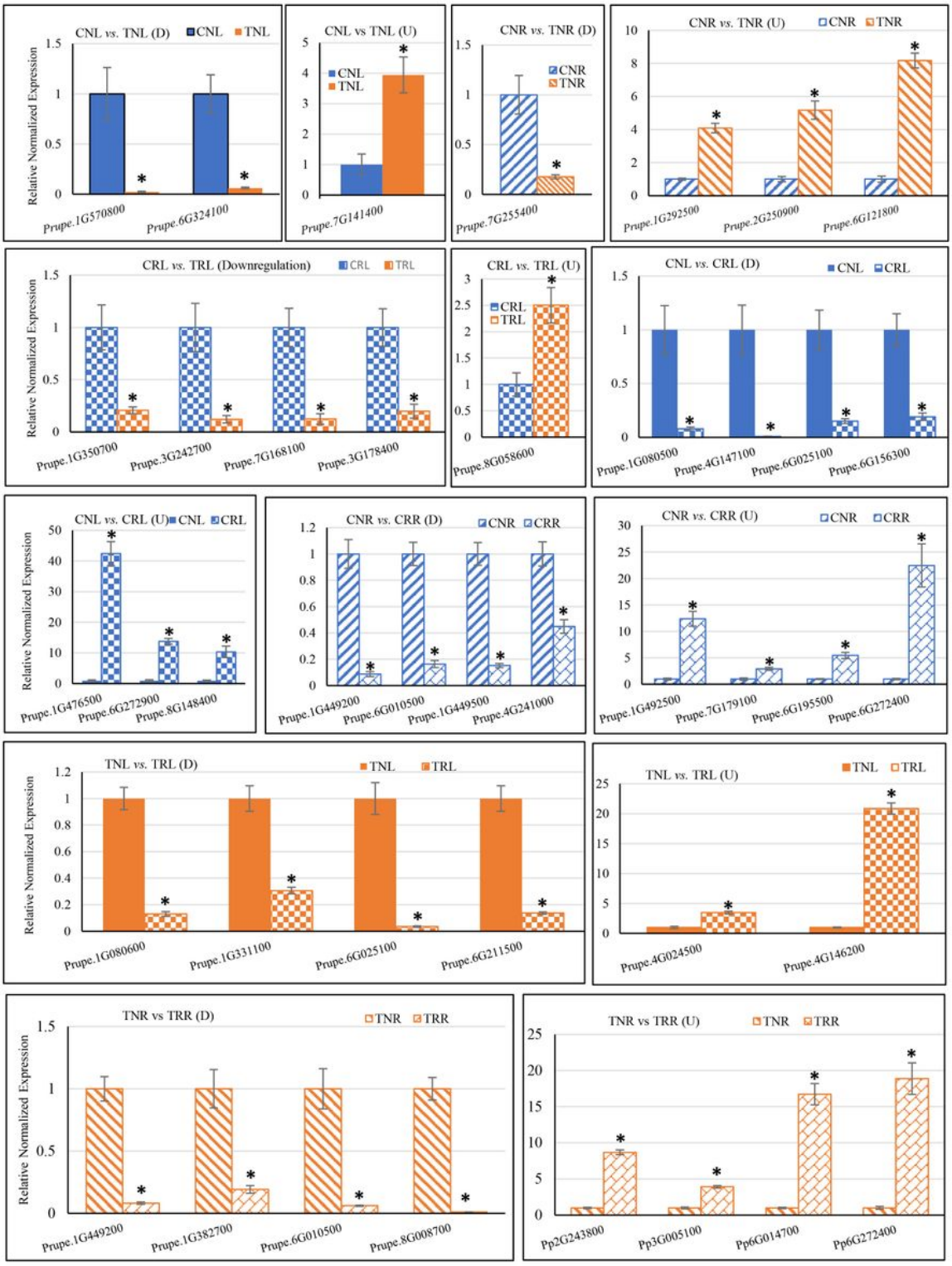

Figure 3

qRT-PCR validation of gene expression observed in RNA-Seq data. The Y-axis indicates relative normalized expression, and the X-axis indicates gene IDs. D indicates downregulation, and U indicates upregulation. An asterisk (*) indicates a significant difference (t-test $p \leq 0.05$). CNL, Control 'Nemaguard' Leaf; TNL, Treatment 'Nemaguard' Leaf; CNR, Control 'Nemaguard' Root; TNR, Treatment 'Nemaguard'

Root; CRL, Control ‘Rootpac 40’ Leaf; TRL, Treatment Rootpac Leaf; CRR: control ‘Rootpac 40’ root; TRR, treatment ‘Rootpac 40’ Root.

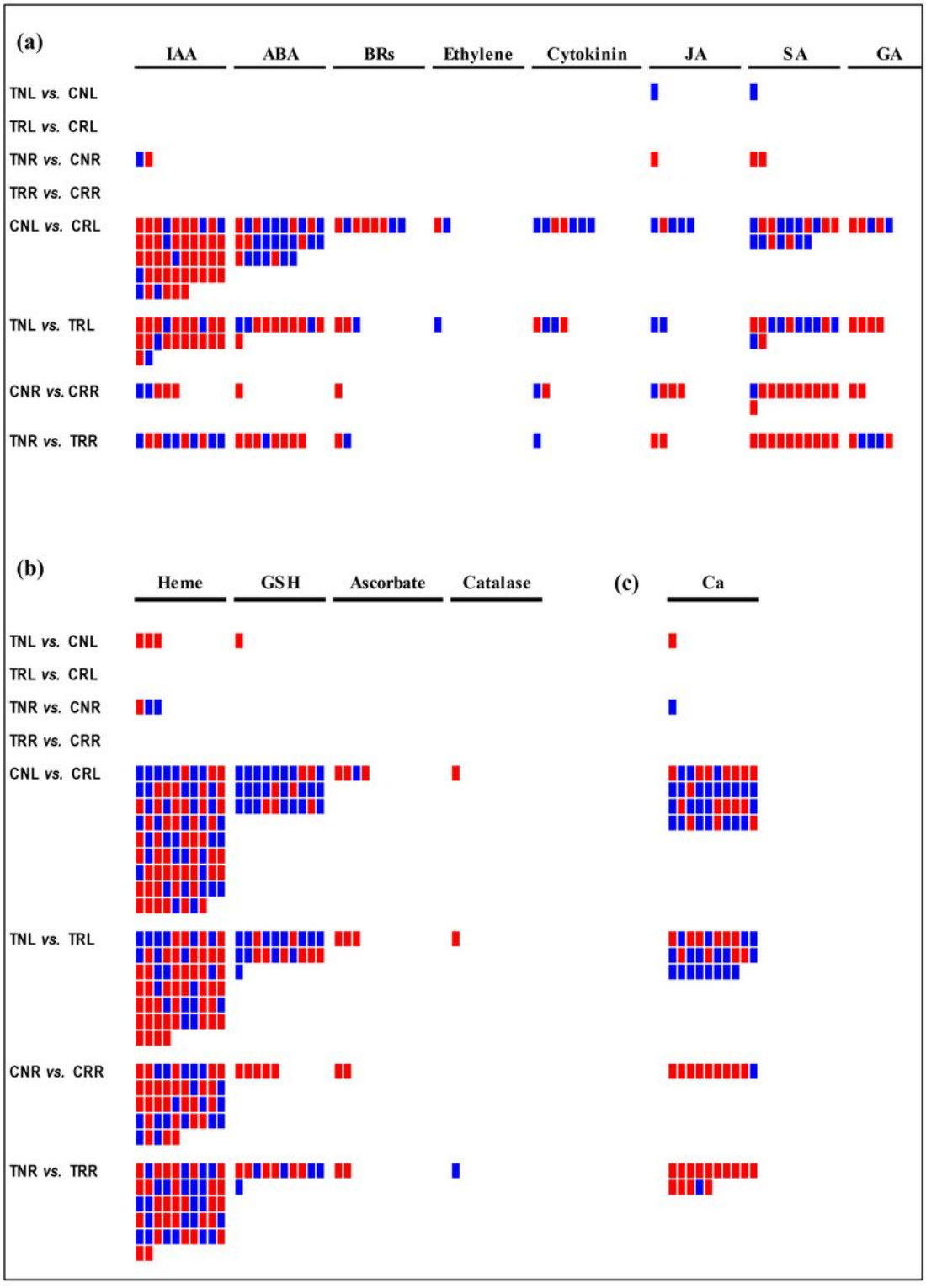

Figure 4

DEGs associated with phytohormone, redox, and calcium signaling pathways. (a) DEGs associated with phytohormone pathways. (b) DEGs associated with redox signaling pathways. (c) DEGs associated with calcium signaling (Ca). The red color indicates downregulated DEGs, and the blue color indicates

upregulated DEGs. Left-side texts show pairwise comparisons. IAA, indole acetic acid (auxin); ABA, abscisic acid; BRs, brassinosteroids; JA, jasmonic acid; SA, salicylic acid; GA, gibberellins; GSH, glutathione; Ca, calcium.

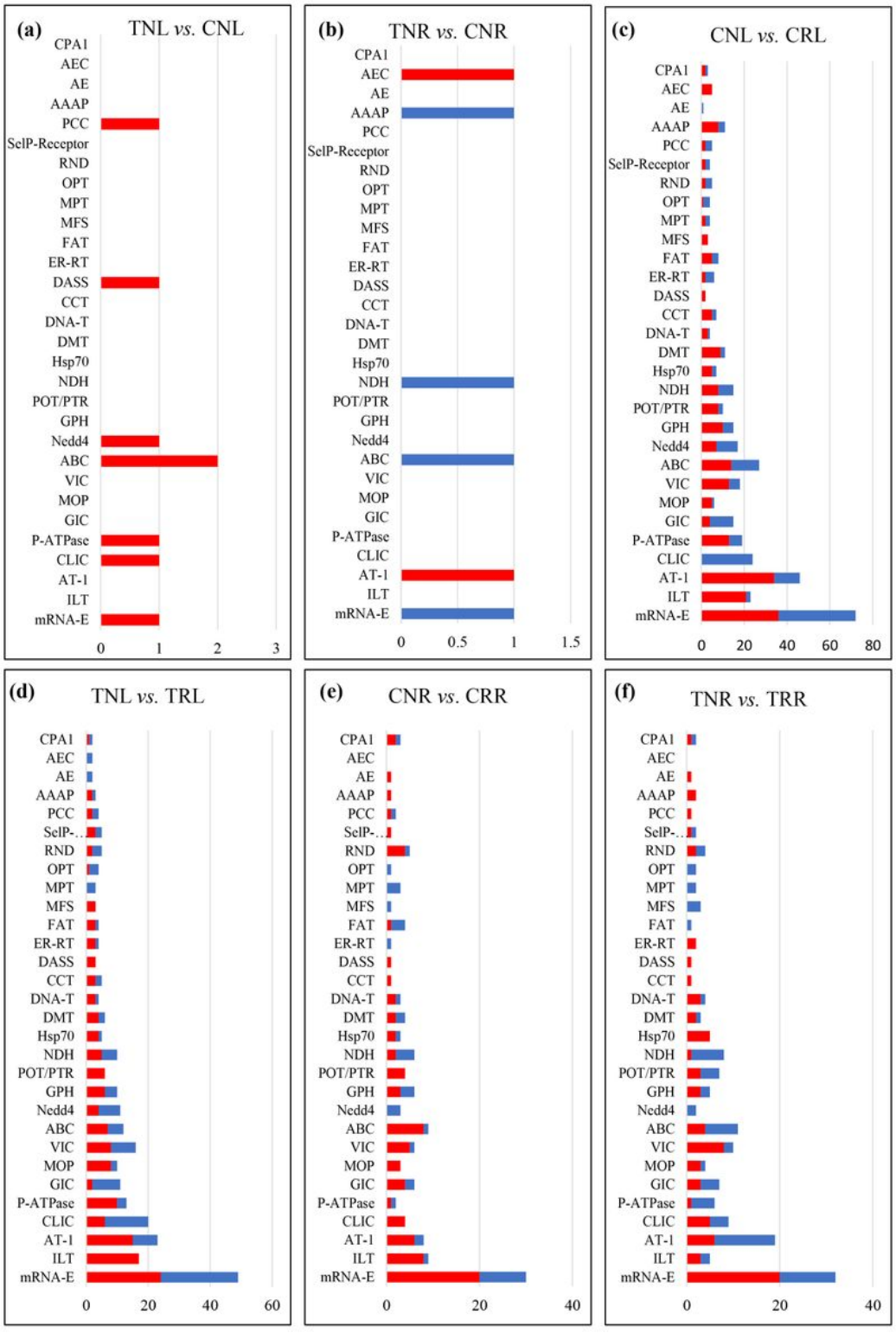

Figure 5

Transporter analysis of DEGs. The Y-axis indicates transporter superfamilies. The X-axis shows gene counts. Salt treatment vs. control comparisons are shown in panel a and panel b. Salt-sensitive vs. salt-

tolerant comparisons are shown in panels c, d, e, and f. The red color indicates downregulated DEGs, and the blue color indicates upregulated DEGs.

Supplementary Files

This is a list of supplementary files associated with this preprint. Click to download.

- SupplementaryFigsBAV4.pdf
- SupplementaryTableS1.docx
- SupplementaryTableS2.xlsx
- SupplementaryTableS3.xlsx
- SupplementaryTableS4.xlsx
- SupplementaryTableS5.xlsx
- SupplementaryTableS6.xlsx
- SupplementaryTableS7.xlsx
- SupplementaryTableS8.xlsx
- SupplementaryTableS9.xlsx
- SupplementaryTableS10.xlsx
- SupplementaryTableS11.xlsx